

HYDROLYTIC AND ENZYMATIC DEGRADATION STUDIES OF BIOMIMETIC SCAFFOLDS FOR BIOMEDICAL APPLICATIONS USING BIORESORBABLE POLYESTERS AND CROSSLINKED COLLAGEN

M. A. Romero ^{a*}, M. A. Sabino ^{b*}, G. González ^c, K. Noris-Suarez ^{a, c}

^aLaboratorio de Ingeniería de Tejidos, Universidad Simón Bolívar, Caracas, Venezuela.

^bGrupo B5IDA, Departamento de Química, Universidad Simón Bolívar, Caracas, Venezuela.

^cLaboratorio de Ciencia e Ingeniería de Materiales, IVIC, Caracas, Venezuela.

^dSchool of Physical Sciences and Nanotechnology. Yachay Tech University. Urcuqui. Ecuador

^eGrupo IBIO. Universidad Internacional de Valencia (VIU), Valencia, España.

*Corresponding authors, E-mail: msabino@usb.ve; mrvivas@gmail.com

Received: 15-08-2023

Accepted: 13-09-2023

Published: 27-09-2023

ABSTRACT

Tissue engineering strategies comprise designing and adapting biomaterials to the physiological requirements of the injured organ or tissue. In some scenarios, biodegradation of the material is necessary to avoid additional surgeries in order to remove remnants of the scaffold. With this objective, we fabricated porous films made with different proportions of polycaprolactone (PCL) blended with polybutylene succinate (PBSucc) and ultra-thin collagen membranes crosslinked with genipin. Fabrication parameters were varied in order to study and propose the best material combinations that will improve the regenerative performance of the films and membranes. In such samples, degradability in physiological conditions was studied and characterized. Spectroscopic, thermal, atomic force (AFM) and scanning electron microscopy (SEM) analyses were additionally carried out. In conclusion, it was proved that both biomaterials analyzed in this investigation were biodegradable, maintaining stability over 40 days in natural ultra-thin membranes and 23 weeks in the synthetic films. These biomimetic matrices offer the possibility of a personalized strategy, appropriate for the regeneration of various types of injured tissues.

Key Words: Biomimetic matrices, Tissue engineering, Biodegradable, Collagen, Polyesters.

ESTUDIOS DE DEGRADACIÓN HIDROLÍTICA Y ENZIMÁTICA DE ANDAMIOS BIOMIMÉTICOS PARA APLICACIONES BIOMÉDICAS UTILIZANDO POLIÉSTERES BIORREABSORBIBLES Y COLÁGENO RETICULADO

RESUMEN

Las estrategias en la ingeniería de tejidos comprenden el diseño y la adaptación de biomateriales a los requisitos fisiológicos del órgano o tejido lesionado. En algunos escenarios, la biodegradación del material es necesaria para evitar cirugías adicionales requeridas para eliminar los restos del andamio. Con este objetivo, fabricamos películas porosas hechas con diferentes proporciones de policaprolactona (PCL) mezcladas con polibutilensuccinato (PBSucc) y membranas ultrafinas de colágeno entrecruzadas con genipina. Se variaron los parámetros de fabricación para estudiar y proponer las mejores combinaciones de materiales que mejorarán el rendimiento regenerativo de las películas y membranas. En dichas muestras se estudió y caracterizó la degradabilidad en condiciones fisiológicas. Además, se llevaron a cabo análisis espectroscópicos, térmicos, de fuerza atómica (AFM) y de microscopía electrónica de barrido (SEM). En conclusión, se comprobó que ambos biomateriales analizados en esta investigación fueron biodegradables, manteniendo su estabilidad durante 40 días en las membranas ultrafinas naturales y 23 semanas en las películas sintéticas. Estas matrices biomiméticas ofrecen la posibilidad de una estrategia personalizada, apropiada para la regeneración de varios tipos de tejidos lesionados.

Palabras clave: Matrices biomiméticas, Ingeniería de tejidos, Biodegradables, Colágeno, Poliésteres.

INTRODUCTION

Biomimetics is a pioneering concept that elicits inspiration from nature and its elements and processes to create solutions to severed health problems [1]. Successful

regeneration of injured tissues can be achieved using various biomimetically designed constructs. In a variety of tissues, studies confirm that biomimetic prototypes must be manufactured from permeable and biodegradable

biomaterials to avoid a second surgical intervention in which the implant must be removed [2]. For example, drug delivery systems, nerve guides, sutures and dressings for wound healing are a few tissue engineering strategies in which biodegradation is highly recommended [3]. However, the material selected must have the ability to orient and preserve cell integrity, avoiding early embrittlement of the structure. Polyesters, alike poly(ϵ -caprolactone) (PCL), offer the advantage of degrading slowly in a physiological environment, which makes PCL an ideal material to use in severed and slow regenerating tissues [4]. In turn, blends of PCL with polyesters of a slightly different chemical composition, such as poly(butylene succinamate) (PBSucc) or poly(ethylene oxide) (PEO), can modulate the resorption rate of scaffolds, adjusting the degradation process to the time required for the restoration of healthy tissue [5, 6]. In addition, to strategies based on synthetic materials, combinations of natural polymers such as collagen, fibrin, chitosan or alginate have been implanted successfully in clinical trials [7]. Some beneficial traits of natural materials are its reticular structure which show similarities with the extracellular matrix and therefore stimulates cellular interaction, high chemical versatility, good biological performance and, enzyme-controlled degradability [8]. In this research, the objective was to evaluate *in vitro* degradation of natural and synthetic matrices which can be used in wound dressing, nerve regeneration and in drug delivery systems. The synthetic matrices were fabricated from porous and non-porous blends of different composition ranges of PBSucc and PCL that should increase controlled degradation in a physiological setting. While natural membranes were fabricated using collagen type I crosslinked with genipin, a natural and non-toxic crosslinking agent. These biomimetic matrices were hydrolytically and enzymatically degraded. Fabrication conditions were varied to study and select the best parameters that will improve the regenerative performance.

MATERIALS AND METHODS

Fabrication of the [PCL_m-PBSucc_n]^z scaffolds

To fabricate the synthetic scaffolds, porous films were produced by using a widely applied method of solvent casting and salt particulate leaching [9, 11]. Briefly, polycaprolactone (PCL; Mw 56,000 Tone 767, Union Carbide) and polybutylene succinate (PBSucc; Mw 23,000 Showa Highpolymer Co. Ltd.) were dissolved in chloroform (3 – 4% w/v) at 60°C. Immediately, salt crystals of NaCl were minced and sieved using a mesh 400 and added to the polymer solutions while stirring. This step was omitted in non-porous samples. Polymer mixtures were poured onto glass plates and placed under ventilation at 25°C to allow solvent evaporation. Salt was extracted stirring films in distilled water and changing medium every 24 hours. The procedure was considered complete when the wash solution presented electrical parameters similar to the ones obtained in pure distilled water, measured using a calibrated electrode [12]. For experimentation, membranes were fabricated using different polymer concentrations with various proportions of PCL-PBSucc and polymer/salt ratios, including non-porous samples (NP). The resulting membranes were identified with the following symbols [PCL_m-PBSucc_n]^z. Fractions of PCL and PBSucc were indicated with a number in the subscript and thickness was identified in the superscript.

Manufacture of ultra-thin collagen gels

Type I collagen was extracted from tendon tissue present in tails of Sprague – Dawley rats, using a modification of the acetic acid protocol [13]. Gel fabrication required the determination of the isoelectric point (pI) in the collagen solution. The pI is the pH at which the overall charge of the protein is zero and it is the point in which collagen molecules organize to form a gel. To do this, volumes of NaOH (1N) and soluble collagen were titrated while measuring simultaneously the pH of the system. The isoelectric point was determined in each new batch of

collagen solution prepared. This method initially required high volumes of the alkaline and collagen solutions. Once the isoelectric point was verified, volumes were adapted to fabricate ultrathin membranes [14].

Genipin cross-linking of ultrathin collagen membranes

Structural stability of the ultra-thin collagen membranes (width $0,02 \pm 0,005$ mm) was increased by crosslinking with genipin using a modified protocol [15]. Briefly, genipin solutions were prepared at 0% (Not-crosslinked, N), 0.05, 0.5, 1.0 and 2.0% w/v, diluting genipin (MW 226.23 g/mol, Challenge Bioproducts) in ethanol and phosphate buffer (20 mM) at pH 7.4. Ultra-thin gels were incubated 5 days at 4 °C in mild motion. Immediately, the genipin/phosphate buffer solution was removed, rinsing samples 4 times in distilled water 30 min each wash. Next, the crosslinked membranes were dried in a laminar flow hood 2 h. Dried membranes (width $0,010 \pm 0,0050$ mm) were stored at 4 °C.

Hydrolytic degradation of [PCL_m-PBSucc_n]^z scaffolds

In vitro hydrolytic degradation of porous and non-porous [PCL_m-PBSucc_n]^z scaffolds was performed simulating physiological conditions using an adapted protocol referenced by the ASTM F1635 norm [16, 17]. In that order, sterilized and moisture-free vacuum-packed samples were incubated in a Ringer – Lactate buffer solution (pH 7.0) at 37°C during a 23-week period after being sealed. Degradation was studied in pieces of identical sizes fabricated with 3 different thickness and 2 distinct polymer/salt ratios. Fresh 20 ml buffer was changed weekly and sterile conditions, while pH values of all solutions were recorded using a pH meter (pH 211, Hanna Instruments). Finally, samples were taken out of the degradation medium, washed gently to remove salts present in the buffer and dried at room temperature. Initial and final weights were compared after the assay was done and changes in the pH of the buffer solutions were presented as delta averages.

Enzymatic degradation of crosslinked collagen membranes

Degradation of crosslinked and non-crosslinked collagen was carried out adapting a previous protocol [18]. Briefly, collagen membranes were cut and weighed using 6 replicates for each type of sample. Such that 4 were subjected to collagenase degradation and 2 served as controls. A type I collagenase purified from *C. histolyticum* (Gibco, Invitrogen) with an activity of 260 U/mg was used to prepare the enzyme solution. Which was resuspended in a TRIS-HCl buffer solution (50 mM pH 7.4) with calcium chloride (10mM, Riedel de Haën PM 110, 9 g/mol), obtaining an activity of 20 U/ml in each well. Meanwhile, control samples were incubated in a similar solution but without collagenase. The samples remained at 37 °C and a pH of 7.5 in a sterile environment for 40 days. The degradation reaction was stopped by adding EDTA (10 mM; ethylenediaminetetraacetic acid MW 292.2 g/mol Scharlau Chemie S.A.) to each well. The degradation medium was changed weekly and at the end of the test the samples were lightly washed in distilled water to remove the salts. Initial and final weights were compared after the assay was done and changes in the pH of the buffer solutions were registered.

Characterization techniques

FTIR

A *Nicolet Magna 750* Spectrometer (Thermo Fisher Scientific) with a DTGS detector and a KBr beam splitter was used at a rate of 32 scans per sample and a resolution of 4 cm⁻¹. Signal deconvolution was obtained in the spectral range of 4000 – 400 cm⁻¹ using a software package (Omnicept, Thermo Electron Corp.).

DSC-TGA

Thermal analysis of [PCL_m-PBSucc_n]^z samples was carried out through Differential Scanning Calorimetry (DSC) in a Perkin-Elmer DSC-7. The equipment was calibrated with an Indium standard, after which 5 mg

samples were tested in aluminum pans under a high purity nitrogen atmosphere. Standard heating and cooling scans were recorded from -10 °C to 100 °C at 20 °C/min. All melting parameters were determined from second heating scans after erasing previous thermal history. Data exploration was carried out using a *Pyris Thermal Analysis Software System* (Pyris 9.1, Perkin-Elmer). The crystallinity percentage (Xc, %) of each component in the samples was estimated according to a widely reported method [19]. Regarding collagen samples, they were processed in an SDT-Q600 equipment (TA Instruments). The conditions for the simultaneous DSC-TGA assay were carried out under an argon environment, at a temperature range from 25 to 600 °C and at a heating rate of 10 °C/min. Thermograms were obtained from the data processed using a software (Q600 V7.0) [5].

Field Emission Scanning electron microscopy (FE-SEM)

FE-SEM was used to analyze pore characteristics and distribution in the samples, also to observe morphological variations in the surface and cross-sectional microstructure after degradation. Briefly, samples processed by cryogenic fracture in liquid nitrogen, were coated with carbon – platinum under a vacuum environment of 10⁻⁶ torr using a sputter coater (Balzers, BAE 301). Later, the coated samples were placed in the vacuum chamber of a FE-SEM (*Inspect F50*, FEI) and viewed at an acceleration voltage of 5 kV.

Atomic force microscopy (AFM) analysis of [PCL_m-PBSucc_n]^z scaffolds

AFM was used to obtain two types of information. First, by phase images, differences in viscoelastic properties of PCL and PBSucc in the polymer blends were confirmed, which also corroborated their distribution in the scaffold. Second, in acoustic mode topographic evidence was obtained of the hydrolytic effect in the samples after degradation. For the analysis, samples were aired clean to remove any particles in the surface. Then placed in the

chamber of an Agilent Technologies 5500 Scanning probe Microscope and viewed at a scanning speed of 2 lines/ sec and a frequency range of 150 – 160 KHz. Images were processed using a software package (Pico Image Basic 5.0.4.5276).

RESULTS

Weight loss determination of [PCL_m-PBSucc_n]^z scaffolds

The hydrolysis rate of the biodegradable scaffolds in a physiological-like environment was investigated. The selected combinations for each sample were non-porous (NP-) films made of [PCL₁₀₀-PBSucc₀]^{0.09}, [PCL₈₀-PBSucc₂₀]^{0.06} and [PCL₈₀-PBSucc₂₀]^{0.10} respectively. Also tested were porous [PCL₁₀₀-PBSucc₀]^{0.16} films fabricated with a 50/50 polymer/salt ratio and [PCL₁₀₀-PBSucc₀]^{0.14} films made with a polymer/salt ratio of 60/40. Five replicas were used for each combination and all the films were assembled into spiral scaffolds before incubation in the buffer (n=5). The percentage of remaining mass of each sample and pH variations in the degradation medium are shown in Fig. 1. It is evident that the observed weight loss is very small, indicating that the materials were resistant to hydrolytic action of the physiological medium after 23 weeks of evaluation. This stability is desirable since these scaffolds were designed for biomedical applications in which restoration of tissue continuity requires a period longer than 6 months.

However, the remaining mass of NP-[PCL₈₀-PBSucc₂₀]^{0.06} and [PCL₈₀-PBSucc₂₀]^{0.10} scaffolds was significantly lower compared to the rest of the samples (98.7 and 98.8% respectively) (p<0.05). These results agree with pH data, especially for the [PCL₈₀-PBSucc₂₀]^{0.06} combination. In this blend, final pH in the buffer was registered at 5.2 possibly indicating a greater diffusion of degradation products from the polymers to the medium in contrast with the other samples [4]. In turn, the non-porous and porous PCL scaffolds fabricated with 50/50 and 60/40 polymer/salt ratios were the most stable having fewer variations in weight and pH.

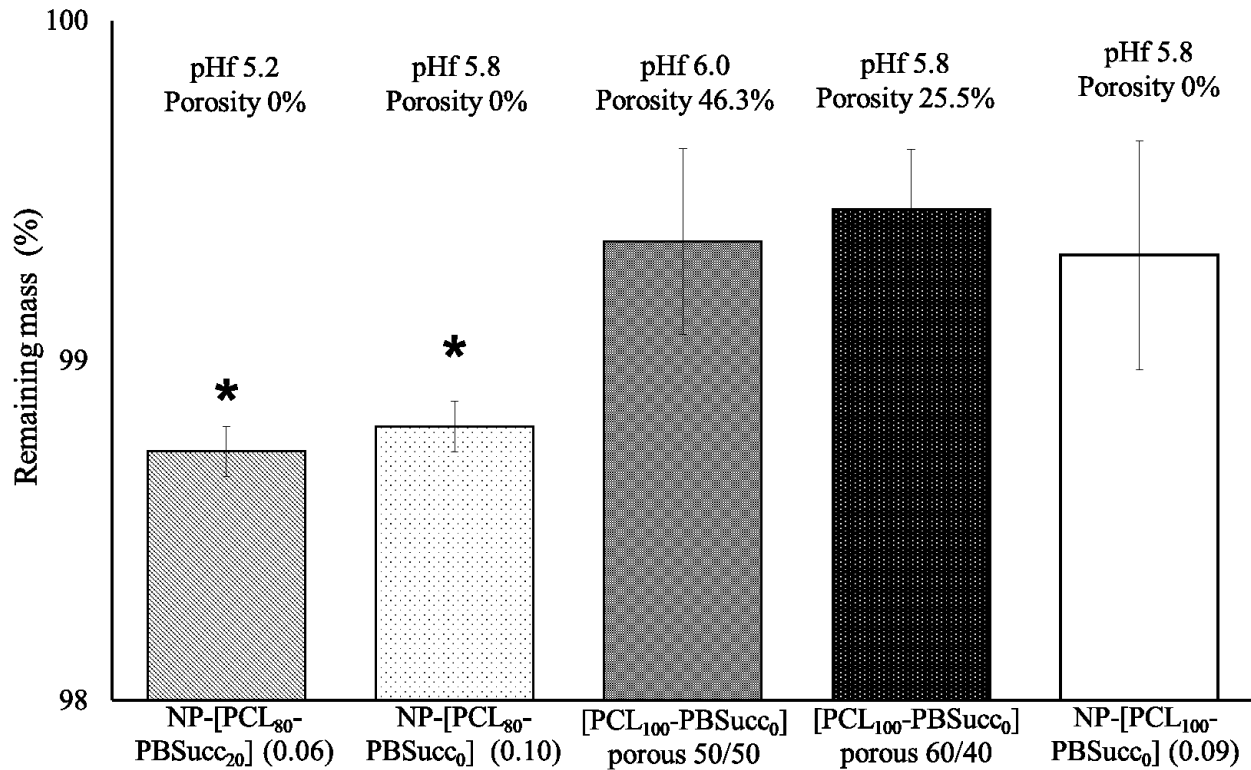


Fig. 1. Percentage of the remaining mass of porous and non-porous samples (NP) after degrading for 23 weeks in a physiological-like medium. Widths of the NP samples were indicated in parenthesis. (*) non-porous combinations [PCL₈₀-PBSucc₂₀]^{0.06} and ^{0.10} were significantly different from the rest of the samples (n = 5). Statistical analysis was performed with a one-way Anova test. Alpha = 0.05.

FTIR analysis of [PCL_m-PBSucc_n]^z scaffolds

Figures 2 and 3 show the FTIR spectrum of samples analyzed in the regions of 1710-1740 and 1100-1220 cm⁻¹ respectively, before and after degradation. Evidence of the hydrolysis process can be found in both regions, as they contain structural information of the carbonyl and carboxylic groups respectively. In Fig. 2, changes in the vibration bands of NP- [PCL₈₀-PBSucc₂₀]^{0.06} samples are perceptible in the 1710 – 1740 cm⁻¹ range after degradation (Fig. 2b, *ii*). In the latter band a modest displacement is noted in the 1735 cm⁻¹ peak corresponding to the vibration of the ester carbonyl group present in the polymers. As the bands in this region show some slight doubling, a Fourier transform deconvolution was performed (results not shown), and it allowed us to verify that indeed, under each signal there were different forms of vibrations,

characteristic of the functional groups that were to be found as hydrolysis products. Also, some increases in the stretching vibrations of the ester carbonyl group subjected to degradation in 50/50 porous [PCL₁₀₀-PBSucc₀]^{0.16} sample (Fig. 2b, *iv*), would seem to confirm that in 23 weeks the chemical environment had begun to change around the polymer functional groups, which is the first effect of hydrolysis prior to mass loss.

In Fig. 3 results were also visible for the NP- [PCL₈₀-PBSucc₂₀]^{0.06} samples. Absorption bands in this range of the spectrum display modifications in the stretching of the symmetric (1050 – 1160 cm⁻¹) and asymmetric (1185 – 1275 cm⁻¹) configuration of the C-O-C groups in the NP- [PCL₈₀-PBSucc₂₀]^{0.06} combination after degradation (Fig. 3b, *ii*).

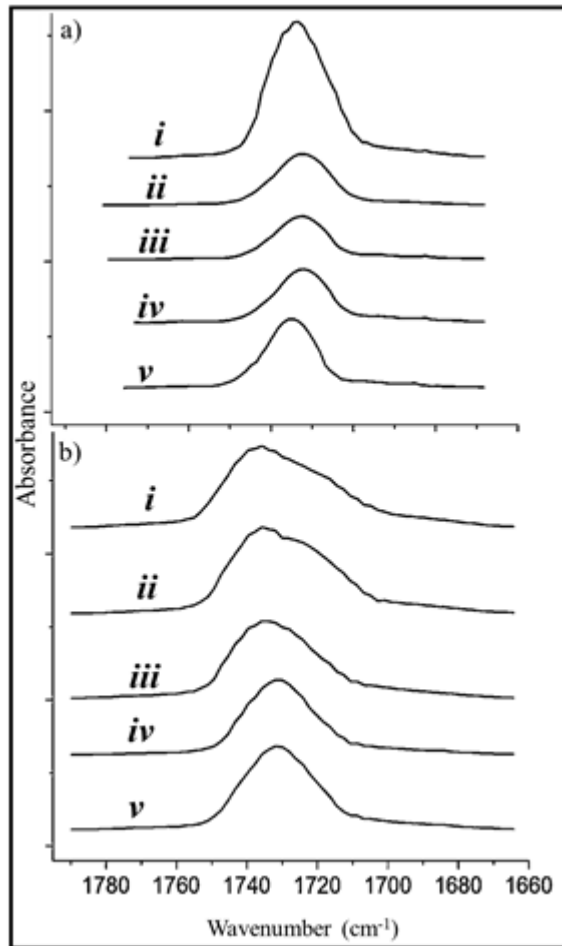


Fig. 2. FTIR spectra in the 1650 – 1750 cm^{-1} region before (a) and after (b) sample degradation. In (a) and (b) combinations were identified as (i) NP- $[\text{PCL}_{80}\text{-PBSucc}_{20}]^{0.10}$, (ii) NP- $[\text{PCL}_{80}\text{-PBSucc}_{20}]^{0.06}$, (iii) NP- $[\text{PCL}_{100}\text{-PBSucc}_0]^{0.09}$, (iv) porous $[\text{PCL}_{100}\text{-PBSucc}_0]^{0.16}$ fabricated with a polymer/salt ratio of 50/50 and (v) porous $[\text{PCL}_{100}\text{-PBSucc}_0]^{0.14}$ fabricated with a polymer/salt ratio of 60/40.

Changes observed in the 1180 - 1345 cm^{-1} and 1205 - 1125 cm^{-1} , suggests that random hydrolysis of the PBSucc in the sample could have generated the appearance of carboxylic acids and alcoholic species. It is also evident, that the rest of the combinations presented only minor chemical modifications after degradation (Fig. 2, 3b, i, iii-v).

DSC thermal analysis of $[\text{PCL}_m\text{-PBSucc}_n]^z$ scaffolds

DSC analyses were carried out to study the thermal behavior after sample degradation, and to compare enthalpy changes between non-degraded $[\text{PCL}_{80}\text{-PBSucc}_{20}]$ polyblends and homopolymeric PCL scaffolds.

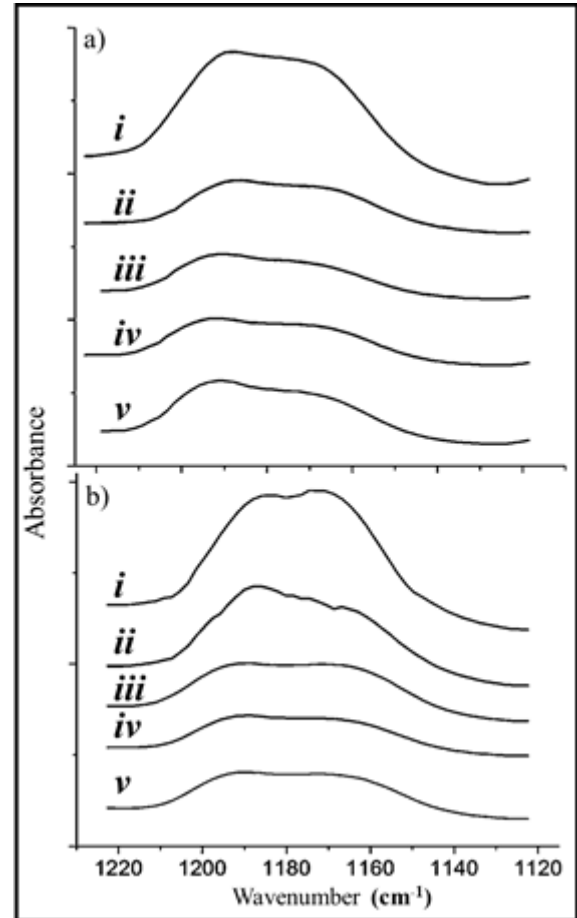


Fig. 3. FTIR spectra in the 1100 – 1220 cm^{-1} region before (a) and after (b) sample degradation. In (a) and (b) combinations were identified as (i) NP- $[\text{PCL}_{80}\text{-PBSucc}_{20}]^{0.10}$, (ii) NP- $[\text{PCL}_{80}\text{-PBSucc}_{20}]^{0.06}$, (iii) NP- $[\text{PCL}_{100}\text{-PBSucc}_0]^{0.09}$, (iv) porous $[\text{PCL}_{100}\text{-PBSucc}_0]^{0.16}$ fabricated with a polymer/salt ratio of 50/50 and (v) porous $[\text{PCL}_{100}\text{-PBSucc}_0]^{0.14}$ fabricated with a polymer/salt ratio of 60/40.

As shown in Fig. 4, samples presented slight modifications in their DSC thermograms after the hydrolytic process, being the NP- $[\text{PCL}_{80}\text{-PBSucc}_{20}]^{0.06}$ combination the most affected by degradation (Fig. 4b, ii). On this matter, cooling and second heating scans of the $[\text{PCL}_{80}\text{-PBSucc}_{20}]$ polyblend displayed a broadening of both the crystallization exotherms and the melting endotherms (Fig. 4 I and II; b, ii). These results are due to the heterogeneous chemical composition of the $[\text{PCL}_{80}\text{-PBSucc}_{20}]$ matrix, and because of the hydrolytic effect on the samples. Note that in the scans the prominent enthalpy curves belong to the PCL fraction. Also apparent, is the

shifting of the PCL and PBSucc crystallization exotherms to a lower temperature (supercooling), more evidently in the hydrolyzed polyblends (Fig. 4, I *b,ii*). Table 1 shows

an increase in the PCL crystallinity percentage (Xc) for all the degraded scaffolds.

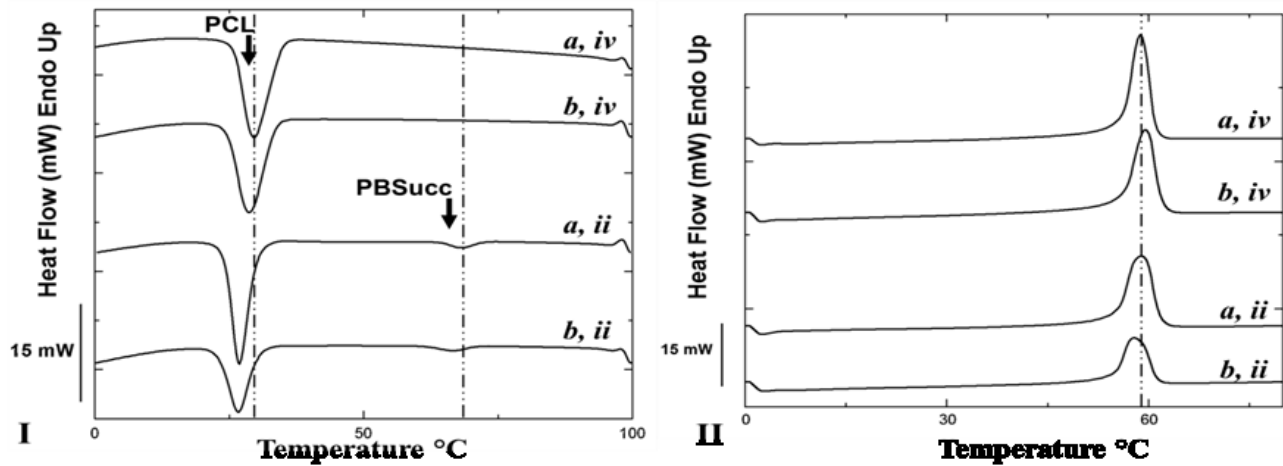


Fig. 4. Standard DSC thermograms. Cooling (I) and second heating (II) scans before (a) and after (b) sample degradation. Combinations in each scan were identified as (ii) NP- [PCL₈₀-PBSucc₂₀]^{0.06} and (iv) porous [PCL₁₀₀-PBSucc₀]^{0.16} fabricated with a 50/50 polymer/salt ratio. Arrows show transitions for PCL and PBSucc fractions.

Table 1 shows an increase in the PCL crystallinity percentage (Xc) for all the degraded scaffolds. On the other hand, the Xc of the PBSucc fraction decreased after hydrolysis of the polyblends. That finding possibly indicates that both the amorphous and crystalline phases of the PBSucc initiated degradation, leaving the PCL polymer remnant in the degraded matrix. This was

corroborated by the increase in the peak melting temperature (Tm) of the degraded NP- [PCL₈₀-PBSucc₂₀] combination, whose value approximated the Tm of the PCL. 50/50 porous [PCL₁₀₀-PBSucc₀]^{0.16} samples presented almost no variations in the DSC scans. Changes of the thermograms in the rest of the combinations were imperceptible.

Table 1. Thermal parameters obtained experimentally of degraded and non-degraded samples of [PCL₁₀₀-PBSucc₀]^{0.16} fabricated with a 50/50 polymer/salt ratio and NP-[PCL₈₀-PBSucc₂₀]^{0.06} polyblends.

Samples	Cooling scan						Second heating scan		
	PBSucc			PCL			PCL		
	Tc	ΔHc	Xc	Tc	ΔHc	Xc	Tm	ΔHm	Xc
[PCL ₁₀₀ -PBSucc ₀] polymer/salt 50/50 ND	-	-	-	28.6	- 63.3	46.5	59.4	65.4	46.9
[PCL ₁₀₀ -PBSucc ₀] polymer/salt 50/50 D	-	-	-	29.6	- 64.3	47.3	58.7	67.8	48.6
NP-[PCL ₈₀ -PBSucc ₂₀] ^{0.06} ND	66.6	-3.3	0.33	26.6	- 39.2	37.0	57.7	40.5	22.9
NP-[PCL ₈₀ -PBSucc ₂₀] ^{0.06} D	68.3	-3.1	0.31	26.9	- 53.4	38.0	59.1	51.9	29.8

(D) degraded; (ND) non-degraded; NP- non-porous; (Tc, °C) peak crystallization temperature; (ΔHc, J/g) crystallization enthalpy; (Xc, %) crystallinity percent; (Tm, °C) peak melting temperature; (ΔHm, J/g) melting enthalpy. Negative values indicate an exothermic process. SD Tc, Tm ± 1°C.

In non-degraded scaffolds, when comparing thermal values between polyblends and homopolymeric samples, table 1 shows a decrease in the crystallization temperatures (T_c) in the PCL fraction. This may be caused by disruptions in the organization of the PCL molecules due to the presence of PBSucc domains scattered in the polymeric matrix that decreased the density of the crystallization nuclei. Additionally, the difference in the crystallization peaks observed in the cooling thermogram is evidence of the immiscibility of both PBSucc and PCL polymers [20].

SEM and AFM morphological characterization of [PCL_m-PBSucc_n]^z scaffolds

Micrographs of the cross-section of a non-porous NP-[PCL₈₀-PBSucc₂₀]^{0.06} scaffold analyzed by SEM are presented in Fig. 5. In these images, distribution of PCL and PBSucc polymers on the wall of degraded and non-degraded samples are displayed (a – f, indicated by *). Results obtained with this technique exhibit no obvious hydrolytic effects on the surface of the material. Thus, to achieve a greater topographic contrast and confirm morphology changes after degradation, samples were analyzed using AFM.

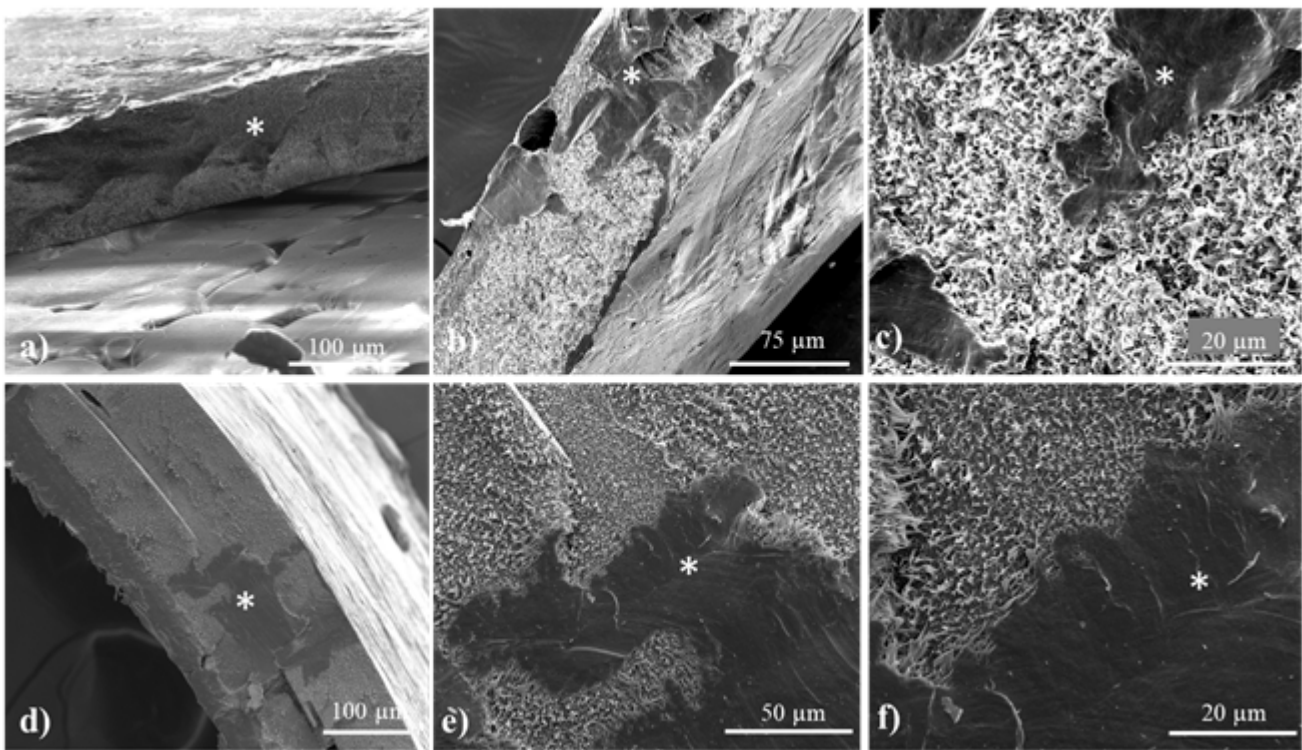


Fig. 5. SEM micrographs of NP- [PCL80-PBSucc20]^{0.06} degraded (a, b and c) and not degraded samples (d, e and f). It is marked with a (*) different polymeric zones probably corresponding to PBSucc. Magnification (a, d) 900X; (b, e) 2000X; (c, f) 5000X.

Fig. 6 displays AFM phase and topographic images of the degraded NP- [PCL₈₀-PBSucc₂₀]^{0.06} combination. In these images' grooves on the surface of the material can be detailed (indicated by arrows). This morphology may have been caused by an erosive effect of the medium and is

possibly the product of an early degradation of the amorphous regions present in both the PBSucc and PCL fractions. It is important to consider that the AFM technique allows to visualize surfaces with distinctive viscoelastic characteristics of the material through phase

images. Phase (Fig. 6 a, c) and topographic images (Fig. 6 b, d) are shown of the undegraded and degraded materials. Therefore, when analyzing images in Fig. 6 it can be inferred that such contrasts are due to the presence of polymers with different compositions in each region (dark or bright) or to amorphous or crystalline regions.

Since the proportions of both polymers are known, the smaller quantities of PBSucc are possibly detailed in reduced areas of the image (Fig. 6 a, c indicated by arrows). Conversely, brighter regions can be assigned to the PCL fraction.

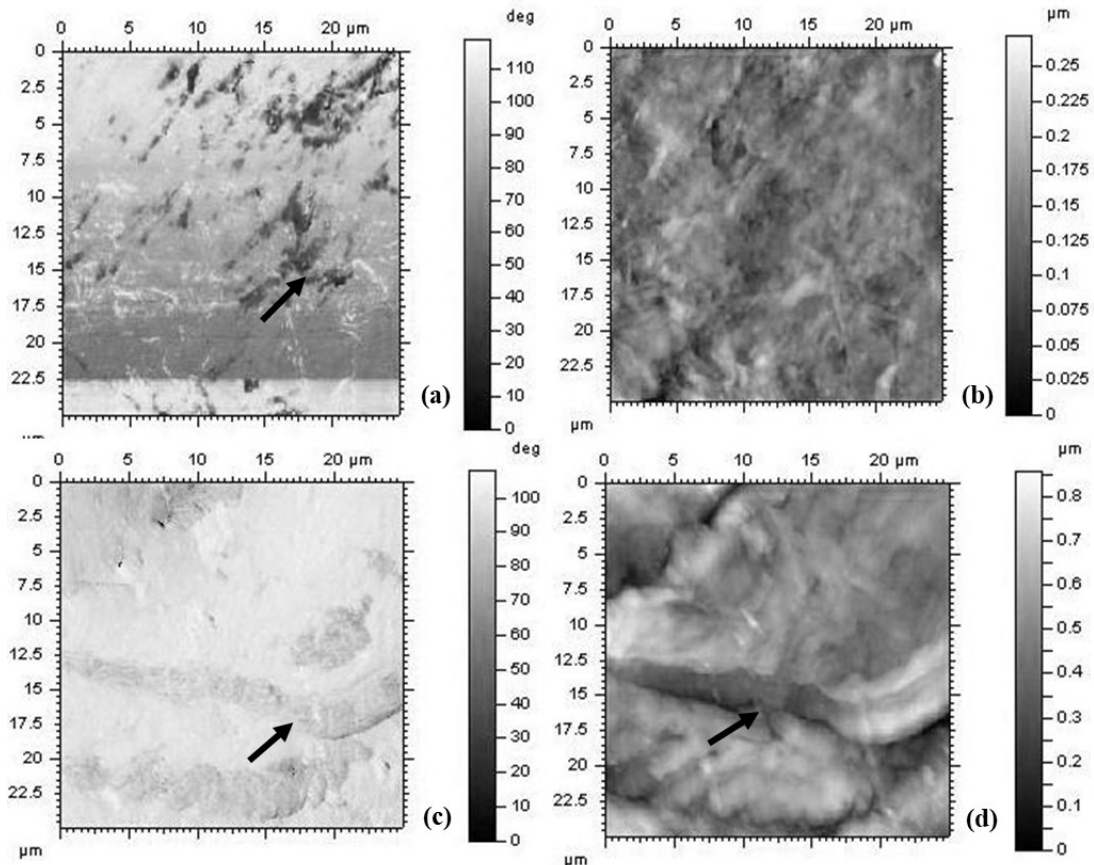


Fig. 6. AFM micrographs of NP- $[PCL_{80}\text{-}PBSucc_{20}]^{0.06}$ samples. Phase (a, c) and topographic images (b, d). Before degrading (a, b) and after degrading (c, d). Arrows indicate the presence of materials with different viscoelastic characteristics that could correspond to PBSucc or amorphous regions in the PCL. Scale bars 20 x 20 μm .

Microscopy techniques confirmed that $[PCL_m\text{-}PBSucc_n]$ mixtures exhibit phase separation, which allows water to penetrate in the polymeric interfaces where there is less molecular order favoring hydrolysis [21].

Degradation of crosslinked and non-crosslinked collagen membranes

This assay was based on the use of a bacterial collagenase to analyze the degradation of crosslinked and non-

crosslinked matrices. It is worth noting that various authors report that the enzyme of bacterial origin has an activity very similar to that described in collagenases isolated from mammals, even correlative results have been reported when carrying out comparative experiments with both proteases [22]. Regarding the non-crosslinked (N) and 0.05% w/v genipin crosslinked membranes, it is necessary to mention that their characterization was not possible, due to their rapid degradation after incubating

them with the enzyme. For this reason, the use of these matrices in a prototype was considered inappropriate. However, the non-degraded samples (N) were included in the successive experiments as a control.

Weight loss determination of crosslinked and non-crosslinked collagen membranes

The degree of structural susceptibility of the collagen samples, crosslinked and non-crosslinked (N), subjected to solutions with collagenase and without collagenase, was followed by weight loss. Membranes subjected to solutions without collagenase presented little variations in their mass and macroscopic integrity at the end of the test

(Fig. 9, a). It can be concluded that the biological polymer samples were not susceptible to the hydrolytic effect of the medium, in the absence of the enzyme, at the end of 40 days at 37 °C (pH 7.5). On the contrary, those samples subjected to the same test solution in which the collagenase was added, showed important losses of their remaining mass (Fig. 7). Thus, the (N) membranes completely dissolved 4 h after starting the assay, while the samples treated with 0.05% w/v completely degraded after approximately 7 days.

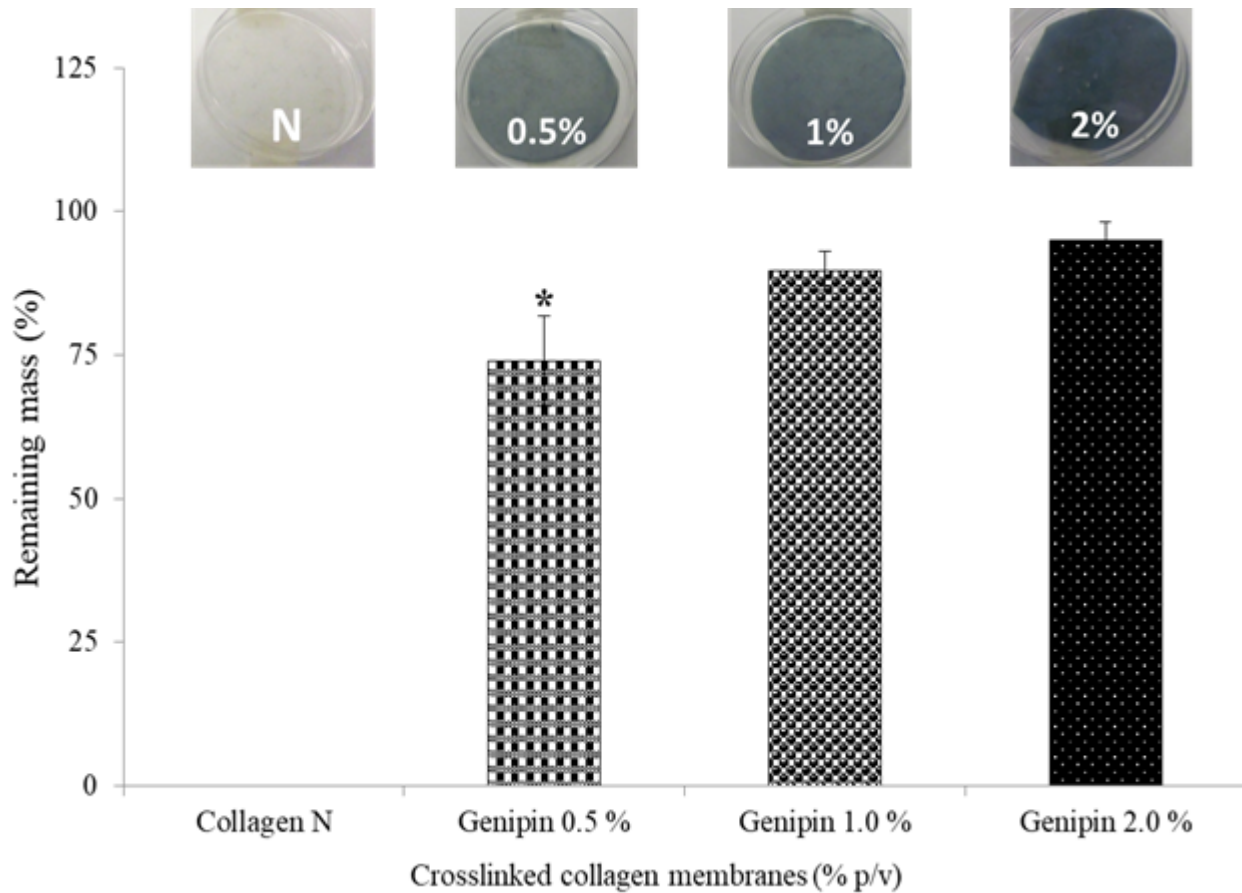


Fig. 7. Percentage of mass remaining in the non-crosslinked (N) and crosslinked membranes after degrading 40 days in a medium similar to the physiological one under the enzymatic action of a commercial collagenase. The membrane treated with 0.5% w/v (*) was significantly different from the rest of the samples. Statistical analysis was performed with a one-way Anova test. Alpha = 0.05, n = 3.

Samples crosslinked with 0.5, 1.0 and 2.0% w/v presented greater stability, reporting mass losses of 26, 10

and 5% respectively (Fig. 7). It was also verified that these samples maintained their macroscopic and microscopic integrity at the end of the 40 days of degradation (Fig. 8 a, c). It is worth noting that the 0.5% w/v crosslinked membranes showed significantly less remaining mass ($p < 0.05$) compared to those crosslinked at 1.0 and 2.0% w/v. However, at the end of the 40 days trial, 0.5% w/v

membranes retained approximately 74% of its mass. While the samples treated with 2.0% w/v showed greater resistance to the protease action maintaining almost 100% of their mass

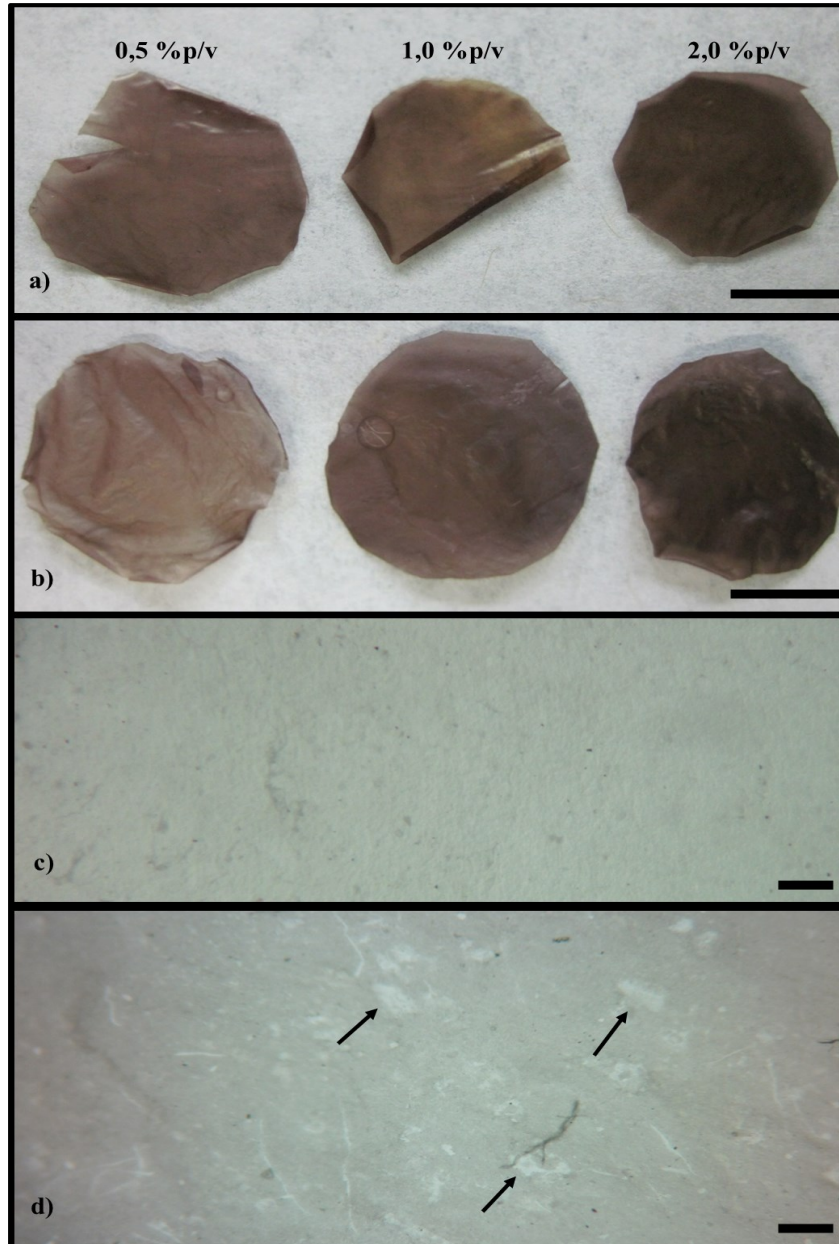


Fig. 8. Photos (a, b) and micrographs (c, d) of membranes cross-linked with 0.5, 1.0 and 2.0% w/v genipin. (a) membranes subjected to the solution without collagenase, (b) membranes subjected to collagenase after 40 days of incubation. In (c and d) samples crosslinked with 0.5% w/v genipin, without collagenase (c) with collagenase (d), arrows point to light areas in the degraded matrix. Images taken with a stereoscopic microscope after 40 days of testing. Scale (a–b) 7.5mm; (c–d) 2mm, 4X magnification.

FTIR analysis of crosslinked and non-crosslinked collagen membranes

To characterize the chemical changes presented by the degraded membranes, an FTIR analysis of the crosslinked samples with 0.5 and 1.0% w/v of genipin was carried out. This is because these combinations were considered the best option for biomedical applications in complex lesions

(easy mechanical manipulation and appropriate mass remaining percentage).

It is important to highlight that the main changes in the 0.5 and 1.0% w/v genipin crosslinked samples were observed in the band located between 1620 - 1700 cm^{-1} , while the rest of the spectrum remained unchanged between the samples.

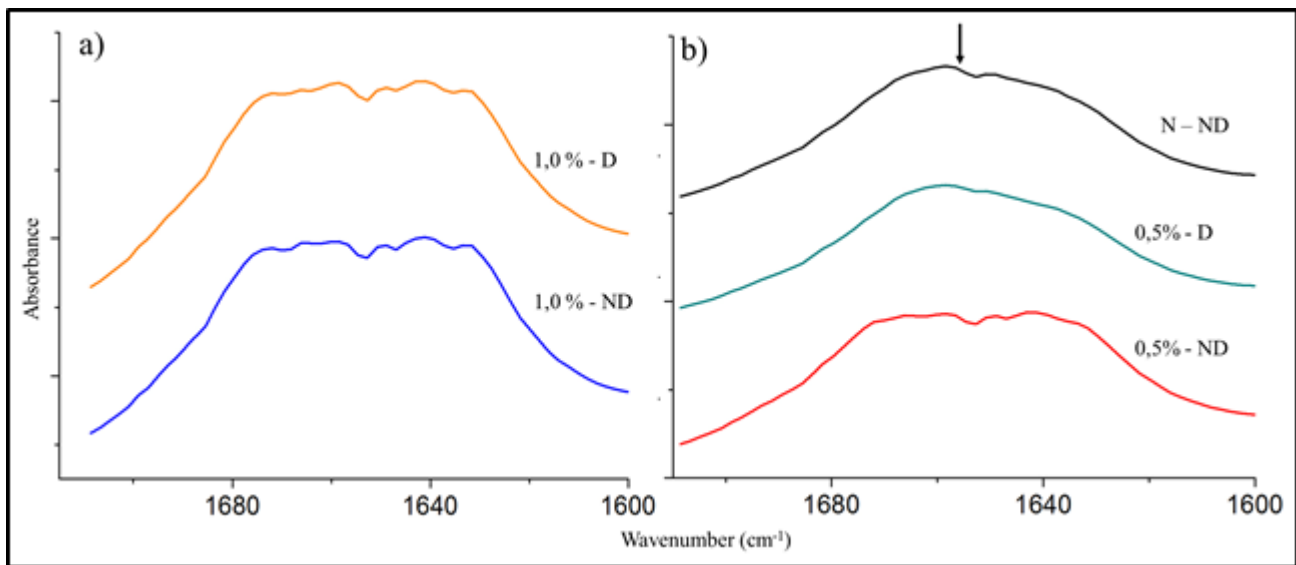


Fig. 9. (a) FTIR spectrum of non-crosslinked (NE) and non-degraded (ND) collagen membranes (black) and degraded (D) (green) and non-degraded (ND) crosslinked collagen at 0.5% w/v (red) in the region 1600 – 1700 cm^{-1} . (b) spectrum of the undegraded (ND) (blue) and degraded (D) (orange) 1.0% w/v crosslinked collagen membranes in the 1600 – 1700 cm^{-1} region.

The effect of the enzymatic action on the 0.5% w/v cross-linked membranes can be detailed in Fig. 9. This process generated evident changes in the band from 1600 to 1700 cm^{-1} due to the enzymatic cleavage on the collagen molecules.

The disappearance of the double absorption band is observed at 1640 – 1660 cm^{-1} in this crosslinked combination, so that it acquired a diffuse shape more similar to that of undegraded non-crosslinked collagen. In turn, the deconvolution obtained in this sample presented

a slight intensity in comparison with the non-crosslinked and non-degraded samples, highlighting that the forms of vibration were similar to that of non-crosslinked collagen (data not shown). It can be verified that in the crosslinked samples at 1% w/v there are few variations between the spectrum of the degraded membrane and that obtained from the non-degraded one (Fig. 9).

DSC – TGA thermal analysis crosslinked and non-crosslinked collagen membranes

Through the calorimetric analysis it was possible to confirm that the degradation generated changes in the thermal behavior of the tested samples (Fig. 10). Among the changes indicated, it was found that the digested samples showed an evident widening of the second energy transition in the membrane treated with 0.5% w/v of genipin. This exotherm is in the temperature range between 150 – 233 °C. As previously reported, this indicates that the 0.5% w/v degraded samples presented a heterogeneous molecular composition compared to the non-degraded ones [18].

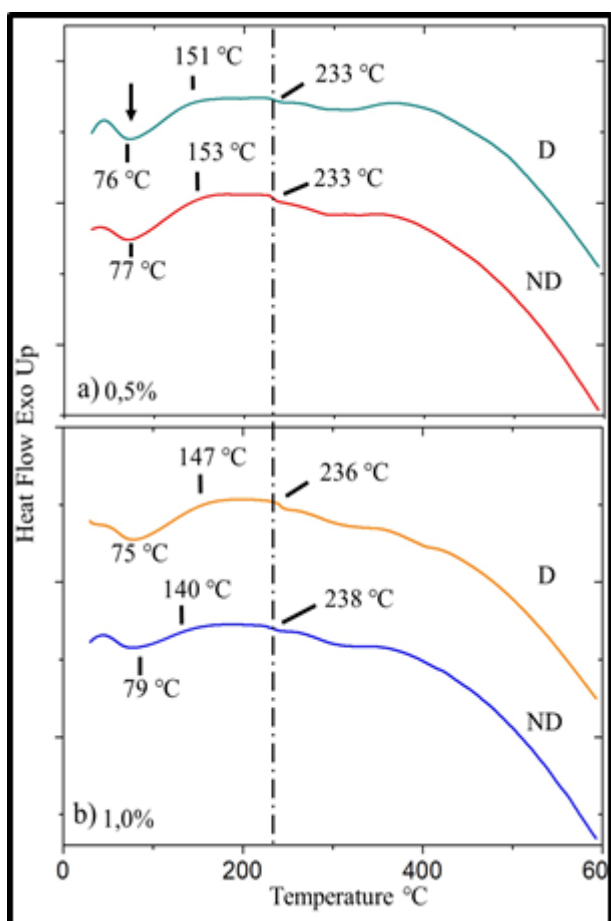


Fig. 10. Standard heating thermograms. (a) Degraded (D, green) and non-degraded (ND, red) membranes, 0.5% w/v genipin crosslinked. (b) the membranes cross-linked with 1.0% w/v not degraded (ND, blue) and degraded (D, orange) are presented.

Which is probably because the enzyme managed to cleave and disrupt the organized structure of the membrane. A similar behavior seems to be repeated in the matrices treated with 1% w/v of genipin, but at a lower intensity. Additionally, it can be deduced that there is a thermal instability, due to the degradation in both samples, which is verified with the decrease in the denaturation temperatures in the first endotherm, from 77 to 76 °C for the crosslinked membranes at 0.5 %w/v and from 79 to 75 °C for those combinations at 1% w/v.

It is possible that the results described, are due to the degeneration of the tropocollagens that constitute the biological polymer, which, when losing their structural organization, probably present an energetic instability. In this sense, the enzyme when making cuts in the triple helix possibly caused the release of bound and structural water present in the collagen. In turn, promoting the formation of random peptides that still remained integrated into the sample at the time of the test [23, 24].

SEM morphological characterization of collagen degradation

The SEM analysis was carried out to analyze the effect of enzymatic degradation on the surface of the samples cross-linked with genipin at 0.5 and 1% w/v.

In Fig. 11, different morphologies can be verified both on the surface and on the edges of the degraded and non-degraded samples. Micrographs (c and d) show the presence of discontinuity spaces, possibly due to random cleavage of the collagenases. These spaces increased in size as the protease eroded the protein and released the peptides that made up the matrix. On the contrary, in the transverse areas of the membrane, fibers are observed that protruded from the edge of the sample, which are probably peptide segments in the process of degradation and released into the aqueous medium.

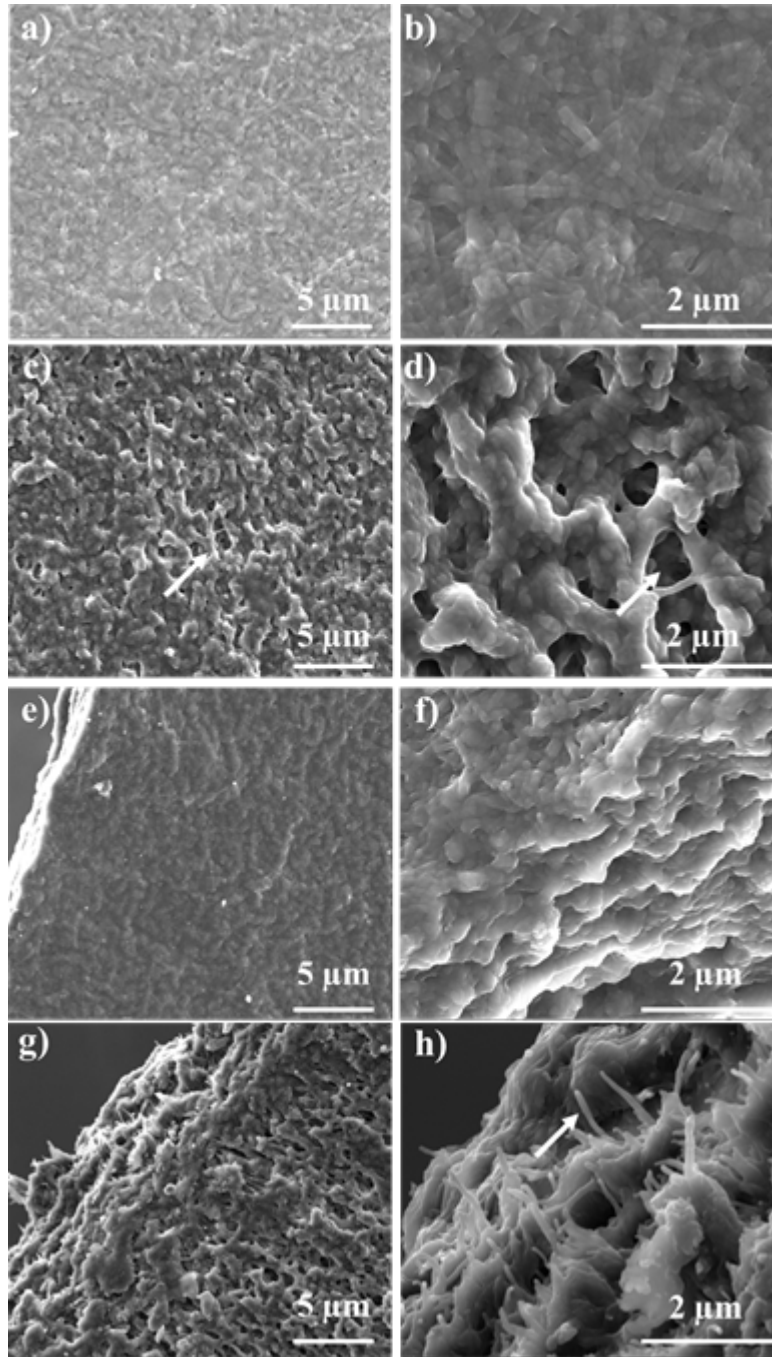


Fig. 11. SEM micrographs of non-degraded (a, b; e, f) and degraded (c, d; g, h) 0.5% w/v crosslinked collagen samples. In (a) and (b) the compact and organized surfaces of the non-degraded matrices are observed. In (c) and (d) the degraded samples are displayed, detailing open spaces of different sizes (arrows). Figures (e) and (f) show the homogeneous edges of the non-degraded matrices. On the contrary, in (g) and (h) it was possible to verify that the edges of the degraded membranes are irregular and fibrous (arrow).

A similar process, but not as marked, can be seen in Fig. 12, which details the crosslinked samples with 1% w/v of genipin, degraded (a – c) and non-degraded (d – f). In this

figure, it can be seen that the surfaces of the degraded matrices are more homogeneous and the open spaces, probably generated by the enzymatic action, are less

evident. In turn, the edges of such samples do not exhibit a highly fibrous appearance, as in the 0.5% w/v genipin treated membranes, such that some collagen strands can barely be seen in the image (12, c arrow). The results seem to indicate a greater resistance to digestion by the crosslinked samples at 1% w/v compared to the matrices treated with 0.5% w/v of genipin. It is worth noting that in

all the micrographs a deposit of salt on the collagen fibers was observed. This precipitate, surely coming from the medium used for the test, prevented a higher resolution in the analysis of the samples.

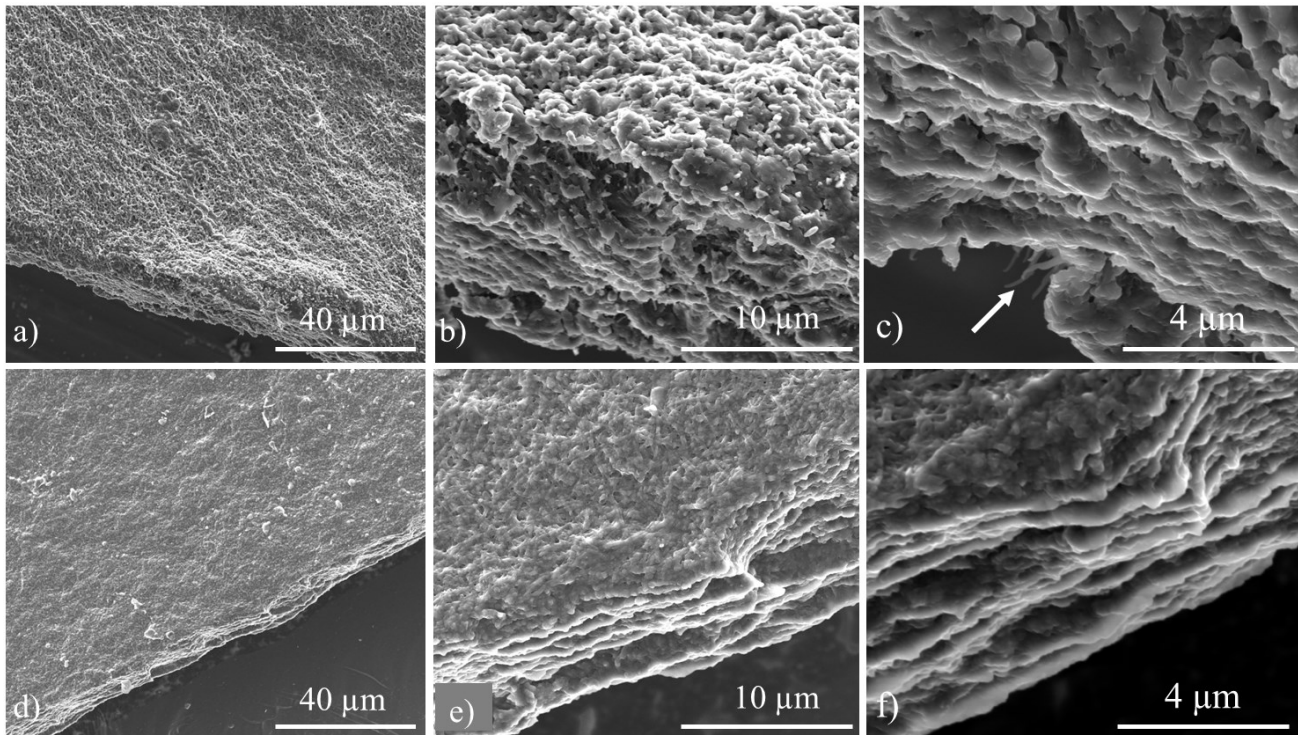


Fig. 12. Micrographs taken by SEM of the degraded (a – c) and non-degraded (d – f) 1.0% w/v crosslinked collagen samples. The images evidence the morphological uniformity of the cross-linked samples subjected to the medium with collagenase and without collagenase. The edges in figure (c) of the degraded sample are slightly fibrous, only finding some protruding peptide fibers (arrow).

DISCUSSION

Biodegradation is a desirable trait in many tissue engineering applications thus it avoids a second surgery to remove the implant. In this study, resorbable synthetic and natural biomimetic matrices were designed and fabricated for multiple biomedical applications. The synthetic porous films, made of different combinations of PCL and PBSucc, were designed to mimic a permeable structural layer capable of protecting growing tissues such as nerve fibers or endothelial lining. On the other hand, the natural membranes crosslinked with genipin were envisioned to

imitate a substrate that could activate and guide cellular growth. In this sense, one of the main objectives in this article was to evaluate the biodegradability of the biomaterials designed in a physiological medium. Results obtained from the synthetic films suggests that resorption may be related to properties such as hydrophilicity and wettability of the polyesters used in their fabrication. These properties were considered owing that hydrolysis in an aqueous solution is the main mechanism of polymer resorption in a physiological environment. It is well documented that hydrophobicity diminishes the

susceptibility of the material to the hydrolytic effect of the medium, while hydrophilicity can catalyze degradation [20]. PCL and PBSucc are hydrolytically labile due to ester bonds, while the predominance of hydrophobic aliphatic chains in their structure makes them stable in an aqueous medium. Based on this, we aimed to synchronize scaffold resorption in a way that tissue would be harbored during regeneration, but also avoiding an additional surgery to remove it after the process is completed. In this work, the period established for the degradation assay was not sufficient to observe a drastic change in mass. This led us to conclude that the stability of the scaffolds in a physiological environment makes them good candidates for long-term applications. However, to avoid the permanency of the implantable device, the use of [PCL_m-PBSucc_n] combinations would be the best option considering they were the most susceptible to hydrolysis and should degrade in a suitable time interval. This could be attributed to a higher wettability degree of the PBSucc which augmented the susceptibility of the polyblends to the hydrolytic effect of water in comparison to the more hydrophobic samples fabricated only with PCL. About degradation of the porous PCL scaffolds, we had hypothesized that porosity should accelerate surface erosion since interconnected pores offer a higher contact-surface with the buffer increasing the possibility of water cleavage towards the ester bonds. Conversely, it was found that such parameter did not significantly affect the degradation rate of the homopolymeric samples possibly due to the highly hydrophobic characteristics of PCL. The hydrophobicity of PCL could have limited the water uptake, and therefore the interaction of the aqueous medium with the scaffolds reducing the rate of hydrolysis [4, 5, 25].

A notable aspect of our prototypes is that pH values of the medium presented only small variations. This is important considering that acidic by-products of the hydrolytic breakdown can lead to an inflammatory response. Slight changes in the pH should minimize inflammation

reactions and reduce the probability of rejection from the host [26].

Summarizing, changes in the crystallinity, melting peaks and in the FTIR spectrum of the degraded synthetic film, were possibly a consequence of the chain scissions of hydrolytically unstable ester bonds located in the amorphous region [4].

Regarding the degradation of the natural polymer, it can be concluded that membranes made of collagen are not susceptible to hydrolysis in the absence of proteases and it is considered that only under enzymatic action can they be resorbable. One family of such enzymes are collagenases, which are essential proteases in tissue repair [23]. Since collagenases are profusely secreted during traumatic events, it is convenient to cross-link samples with genipin concentrations greater than 0.05% w/v and less than 2.0% w/v in order to prolong the membrane stability. It should be mentioned, that for this last combination, negative results were obtained due to its poor handling flexibility and tendency to fold. Therefore, the use of cross-linked membranes with 0.5 and 1.0% w/v genipin is suggested. In regards to the chemical and calorimetric results, changes reflected in the degraded collagen membranes, may be due to the enzymatic action of the collagenases, which are capable of making cuts in the collagen triple helix, generating multiple small and random peptides that will be released into the medium [18]. Collagenases are capable of breaking peptide bonds, which are amide-type bonds, specifically in the regions made up of Proline-X-Glycine-Proline-Y. As reported in previous studies, the process begins at the superficial level and at the edges of the samples, such that the protease will erode towards deeper layers of the membrane [27]. In the case of genipin cross-linked membranes, degradation results may be explained by 3 possibilities. The first one, is that the concentration of 1% w/v was high enough to penetrate deeper areas of the sample, managing to crosslink the internal fibers in the matrix, which remained stable under

enzymatic action. This concentration was also high enough to offer resistance to the enzymatic action on the surface, due to better masking of the cleavage points of the enzyme. The second proposal suggests that the crosslinking mechanism was superficial, especially for lower concentrations of genipin, such that the surface was crosslinked while the core of the membrane was not. A third proposal is that crosslinking with genipin generates amide bonds in the collagen gel, for which collagenase are specific. The presence of larger amounts of amide bonds in crosslinked samples, saturated the catalytic activity of the enzyme, slowing down the degradation of non-crosslinked areas. That is why 0.5%w/w samples showed a characteristic spectrum very similar to that of collagen (N) after degradation, but with less intensity due to the cleavage of amide bonds by protease action.

CONCLUSION

Both synthetic and natural matrices were susceptible to biodegradation, hydrolytically and enzymatically. The biomaterials proposed in this study can be adapted to the requirements of the lacerated tissue. Combinations of [PCL_m-PBSucc_n]^z scaffolds were more susceptible to degradation in comparison to homopolymeric PCL samples. It is necessary to stabilize collagen matrices with a crosslinker to guarantee an optimal performance in tissue regeneration. The tested parameters show that both the natural polymer membranes and the synthetic polymer scaffolds have various long-term and short-term applications.

ACKNOWLEDGMENT

This work was financed by funds granted by the LOCTI-USB-FUNINDES Project No. 5894-08, entitled "Development of Nervous System grafts, using tissue bioengineering". Dr. Sabino wants to thank the academic vice-rectorate of the USB for his sabbatical leave; and FAPESP (SP, Brazil) process # 2021/13949-5 for financial

support during his sabbatical year at CTI Renato Archer (Campinas, SP).

CONFLICTS OF INTEREST

The authors declare no conflict of interest.

REFERENCE

- [1] P. Thanigaiarasu (2020) "Biomimetics in the design of medical devices," in *Trends in Development of Medical Devices*, P. B. Prakash Srinivasan Timiri Shanmugam, Logesh Chokkalingam, Ed. Academic Press, pp. 35–41.
- [2] B. Kuang, G. Pena, P. Cowled, R. Fitridge, J. Greenwood, and M. Wagsta (2022) "Use of Biodegradable Temporising Matrix (BTM) in the reconstruction of diabetic foot wounds : A pilot study," *Scars, Burn. Heal.*, vol. Sep 21, no. 8:20595131221122272, doi: 10.1177/20595131221122272.
- [3] M. Modrák, M. Trebunová, A. Findrik, R. Hudák, and J. Živcák (2023) "Biodegradable Materials for Tissue Engineering : Development , Classification and Current Applications," *J. Funct. Biomater.*, vol. 14, no. 159, pp. 1–21.
- [4] A. Leroux, T. N. Nguyen, A. Rangel, D. G. Castner, I. Cacciapuoti, and D. Duprez (2020) "Long-term hydrolytic degradation study of polycaprolactone films and fibers grafted with poly (sodium styrene sulfonate): Mechanism study and cell response," *Biointerphases*, vol. 5, no. 1, pp. 1–15, doi: 10.1116/6.0000429.
- [5] G. S. N. Bezerra, G. G. De Lima, D. M. Colbert, E. Halligan, J. Geever, and L. Geever (2023) "Micro-Injection Moulding of PEO/PCL Blend–Based Matrices for Extending Oral Delivery of Fenbendazole," *Pharmaceutics*, vol. 15, no. 3, doi: 10.3390/pharmaceutics15030900.
- [6] L. Yu, F. Wang, and S. Huang (2023) "Fabrication and Properties of Polycaprolactone / Poly (Butylene Succinate) Blends Based on Electrospinning," *Int. J. Polym. Sci.*, vol. 2023, p. 12, doi: /doi.org/10.1155/2023/9471371.
- [7] H. M. Nguyen et al. (2023) "RSC Advances Biomedical materials for wound dressing : recent advances and applications," *RSC Adv.*, vol. 13, pp. 5509–5528, doi: 10.1039/D2RA07673J.
- [8] P. B. Malafaya, G. A. Silva, and R. L. Reis (2007) "Natural-origin polymers as carriers and scaffolds for biomolecules and cell delivery in tissue engineering applications," *Adv Drug Deliv Rev*, vol. 30, no. 59, pp. 4–5, doi: 10.1016/j.addr.2007.03.012.
- [9] S. Vijayavenkataraman (2020) "Nerve guide conduits for peripheral nerve injury repair: A review on design, materials and fabrication methods," *Acta Biomater.*, vol. 106, no. xxx, pp.

- 54–69, 2020, doi: 10.1016/j.actbio.2020.02.003.
- [10] L. E. Kokai, Y.-C. Lin, N. M. Oyster, and K. G. Marra (2009) “Diffusion of soluble factors through degradable polymer nerve guides: Controlling manufacturing parameters.” *Acta Biomater.*, vol. 5, no. 7, pp. 2540–50, doi: 10.1016/j.actbio.2009.03.009.
- [11] W. L. Murphy, R. G. Dennis, J. L. Kileny, and D. J. Mooney (2002) “Salt Fusion: An approach to improve pore interconnectivity within tissue engineering scaffolds.” *Tissue Eng.*, vol. 8, no. 1, pp. 43–52.
- [12] J. Reigner and M. A. Huneault (2006) “Preparation of interconnected poly(ϵ -caprolactone) porous scaffolds by a combination of polymer and salt particulate leaching,” *Polymer (Guildf.)*, vol. 47, no. 13, pp. 4703–4717, doi: 10.1016/j.polymer.2006.04.029.
- [13] M. J. O. Francis and M. D. C. (1966) “Extraction of polymeric collagen from human skin.” *Proc. Biochem. Soc.*, vol. 99, no. 1964, pp. 41P-58P.
- [14] M. A. Romero, F. Sánchez, M. A. Sabino, J. P. Rodríguez, G. González, and K. Noris-Suárez (2011) “Biocompatibility study on substrates fabricated for nerve guides using scanning electron microscopy and comparing two drying sample methods.” *Acta Microsc.*, vol. 20, no. 2, pp. 131–140.
- [15] T. A. Shaik et al. (2020) “FLIm and Raman Spectroscopy for Investigating Biochemical Changes of Bovine Pericardium upon,” *Molecules*, vol. 25, no. 17, p. 3857 doi: 10.3390/molecules25173857.
- [16] M. Jayabalan (2009) “Studies on poly (propylene fumarate-co-caprolactone diol) thermoset composites towards the development of biodegradable bone fixation devices.” *Int. J. Biomater.*, vol. 2009, p. 10, doi: 10.1155/2009/486710.
- [17] J. Schachtner, M. Frohbergh, N. Hickok, and S. Kurtz (2019) “Are Medical Grade Bioabsorbable Polymers a Viable Material for Fused Filament Fabrication?,” *J. Med. Device.*, vol. 13, no. September, pp. 1–5, doi: 10.1115/1.4043841.
- [18] B. Kaczmarek-Szczepańska et al. (2023) “The characterization of collagen-based scaffolds modified with phenolic acids for tissue engineering application,” *Sci. Rep.*, vol. 13, no. 1, pp. 1–12, doi: 10.1038/s41598-023-37161-6.
- [19] M. A. Sabino (2007) “Oxidation of polycaprolactone to induce compatibility with other degradable polyesters.” *Polym. Degrad. Stab.*, vol. 92, pp. 986–996, doi: 10.1016/j.polymdegradstab.2007.03.010.
- [20] J. Ostrowska, W. Sadurski, M. Paluch, P. Tyński, and J. Bogusz (2019) “The effect of poly(butylene succinate) content on the structure and thermal and mechanical properties of its blends with polylactide,” *Polym. Int.*, vol. 68, no. 7, pp. 1271–1279, doi: 10.1002/pi.5814.
- [21] L. N. Woodard and M. A. Grunlan (2019) “Hydrolytic Degradation of PCL–PLLA Semi-IPNs Exhibiting Rapid, Tunable Degradation,” *ACS Biomater. Sci. Eng.*, vol. 5, no. 2, pp. 498–508, Feb. doi: 10.1021/acsbiomaterials.8b01135.
- [22] P. Chang, B. Guo, Q. Hui, X. Liu, and K. Tao (2017) “A bioartificial dermal regeneration template promotes skin cell proliferation in vitro and enhances large skin wound healing in vivo,” *Oncotarget*, vol. 8, no. 15, pp. 25226–25241, doi: 10.18632/oncotarget.16005.
- [23] M. Harris, J. Potgieter, K. Ishfaq, and M. Shahzad (2021) “Developments for Collagen Hydrolysate in Biological, Biochemical, and Biomedical Domains: A Comprehensive Review,” *Materials (Basel)*, vol. 14, no. 11, p. 2806, doi: 10.3390/ma14112806.
- [24] M. F. Paige, A. C. Lin, and M. C. Goh (2002) “Real-time enzymatic biodegradation of collagen fibrils monitored by atomic force microscopy.” *Int. Biodeterior. Biodegradation*, vol. 50, no. 1, pp. 1–10 doi: 10.1016/S0964-8305(01)00125-1.
- [25] E. Can, S. Bucak, E. Kınacı, A. C. Çalikoğlu, and G. T. Köse (2014) “Polybutylene Succinate (PBS) – Polycaprolactone (PCL) Blends Compatibilized with Poly(ethylene oxide)- block-poly(propylene oxide)- block-poly(ethylene oxide) (PEO-PPO-PEO) Copolymer for Biomaterial Applications,” *Polym. Plast. Technol. Eng.*, vol. 53, no. 11, pp. 1178–1193, Jul. doi: 10.1080/03602559.2014.886119.
- [26] Z. Xiang, X. Guan, Z. Ma, Q. Shi, M. Panteleev, and F. I. Ataullakhanov (2023) “Bioactive fibrous scaffolds with programmable release of polypeptides regulate inflammation and extracellular matrix remodeling,” *Regen. Biomater.*, vol. 10, no. February, doi: 10.1093/rb/rbad010.
- [27] M. D. Shoulders and R. T. Raines (2010) “Collagen structure and stability.” *Annu Rev Biochem*, vol. 78, pp. 929–958, doi: 10.1146/annurev.biochem.77.032207.120833.CO LLAGEN.